



miR-4759 suppresses breast cancer through immune checkpoint blockade



You-Zhe Lin^a, Shu-Hsuan Liu^b, Wan-Rong Wu^a, Yi-Chun Shen^a, Yuan-Liang Wang^{a,c}, Chien-Ching Liao^a, Pei-Le Lin^a, Han Chang^d, Liang-Chih Liu^e, Wei-Chung Cheng^{a,b,g,*}, Shao-Chun Wang^{a,b,c,f,g,h,*}

^a Graduate Institute of Biomedical Sciences, College of Medicine, China Medical University, Taichung 40402, Taiwan

^b Research Center for Cancer Biology, China Medical University, Taichung 40402, Taiwan

^c Center for Molecular Medicine, China Medical University Hospital, Taichung 40447, Taiwan

^d Division of Molecular Pathology, Department of Pathology, China Medical University Hospital, Taichung 40447, Taiwan

^e Department of Surgery, China Medical University Hospital, Taichung 40447, Taiwan

^f Department of Cancer Biology, University of Cincinnati, Cincinnati, OH 45267, USA

^g Cancer Biology and Drug Discovery Ph.D. Program, China Medical University, Taichung 40402, Taiwan

^h Department of Biotechnology, Asia University, Taichung 41354, Taiwan

ARTICLE INFO

Article history:

Received 21 August 2021

Received in revised form 2 December 2021

Accepted 12 December 2021

Available online 16 December 2021

Keywords:

Breast cancer

Immune checkpoint

miRNA

miR-4759

PD-L1

ABSTRACT

Programmed cell death protein 1 (PD-1)/ programmed cell death protein ligand 1 (PD-L1) is the key immune checkpoint governing evasion of advanced cancer from immune surveillance. Immunotherapy (IO) targeting PD-1/PD-L1 with traditional antibodies is a promising approach to multiple cancer types but to which the response rate remains moderate in breast cancer, calling for the need of exploring alternative IO targeting approaches. A miRNA-gene network was integrated by a bioinformatics approach and corroborated with The Cancer Genome Atlas (TCGA) to screen miRNAs regulating immune checkpoint genes and associated with patient survival. Here we show the identification of a novel microRNA miR-4759 which repressed RNA expression of the PD-L1 gene. miR-4759 targeted the PD-L1 gene through two binding motifs in the 3' untranslated region (3'-UTR) of PD-L1. Reconstitution of miR-4759 inhibited PD-L1 expression and sensitized breast cancer cells to killing by immune cells. Treatment with miR-4759 suppressed tumor growth of orthotopic xenografts and promoted tumor infiltration of CD8⁺ T lymphocytes in immunocompetent mice. In contrast, miR-4759 had no effect to tumor growth in immunodeficient mice. In patients with breast cancer, expression of miR-4759 was preferentially downregulated in tumors compared to normal tissues and was associated with poor overall survival. Together, our results demonstrated miR-4759 as a novel non-coding RNA which promotes anti-tumor immunity of breast cancer.

© 2021 Published by Elsevier B.V. on behalf of Research Network of Computational and Structural Biotechnology. This is an open access article under the CC BY-NC-ND license (<http://creativecommons.org/licenses/by-nc-nd/4.0/>).

1. Introduction

Breast cancer is the most common cancer type and the leading cause of cancer-related death in women [1]. Although initially considered as non-immunogenic, emerging studies have demonstrated the presence of immune infiltrates and that the expression of immune-related genes in primary tumors is associated with favorable outcomes in breast cancer [2].

The immune checkpoints, which are inhibitory receptors to the immune response, are the built-in fail-safe mechanism for main-

taining immune homeostasis in normal cells [3]. In cancer cells, on the other hand, inhibitory checkpoints are often hijacked for pro-tumor immune suppression [3,4]. Many members of the inhibitory checkpoints belong to the B7 family, such as PD-L1, PD-L2, B7-H3, and B7-H4 [5]. Their aberrant expression on cancer cell surface is associated with T cell dysfunction and exhaustion, leading to evading of immune surveillance [3,6]. Immune checkpoint blockade (ICB) therapeutics targeting the inhibitory molecules is a promising strategy in breast cancer treatment. However, across the board, the efficacy of ICB therapies in breast cancer has yet fulfilled the promise [7,8].

It has been shown that the resistance to ICB treatments is mediated by epigenetics, transcriptional, and post-transcriptional regulation [8]. The epithelial-mesenchymal transition induces the expression of STT3, the catalytic subunit of an

* Corresponding authors at: Graduate Institute of Biomedical Sciences, College of Medicine, China Medical University, Taichung 40402, Taiwan.

E-mail addresses: wccheng@mail.cmu.edu.tw (W.-C. Cheng), scpwang@mail.cmu.edu.tw (S.-C. Wang).

oligosaccharyltransferase, and increased PD-L1 N-linked glycosylation in cancer stem cells, leading to PD-L1 upregulation and cancer immune evasion [9]. In addition, activation of receptor tyrosine kinase signaling can also promote immunosuppression function of PD-L1 through glycosylation modification [10]. A CRISPR/Cas9-based screening identified the α -(1,6)-fucosyltransferase FUT8 that catalyzes fucosylation and subsequently upregulates the expression of cell-surface PD-1, resulting in T cell inhibition [11]. In contrast, IL-2 induces the E3 ubiquitin ligase FBXO38 catalyzing proteolytic degradation of PD-1, thus enhancing the anti-tumor activity of the tumor-infiltrating lymphocytes (TILs) [12]. These studies unveil the post-transcriptional plasticity of immune checkpoints and highlight the potential of targeting gene expression in their control in therapeutics.

There is emerging evidence supporting the important roles of miRNAs in the tumor immune microenvironment [13]. miRNAs are small non-coding RNAs that bind to motifs of complementary sequence in the 3' UTR of the target mRNAs and post-transcriptionally suppress their expression [14]. For example, miR-155 directly binds to the 3'-UTRs of CTLA4 and BTLA and decreases their expression, subsequently suppressing the effector functions of CD8⁺ T cells [15,16]. Administration of miR-138 decreases PD-1 and CTLA-4 expression in TILs, which in turn inhibits glioma tumor growth [17]. Deficiency of miR-15a/16 enhances anti-tumor immunity and correlates with reduced expression of TIM-3 and LAG-3 in the tumor-infiltrating CD8⁺ T cells [18]. These studies suggest a miRNA-mediated regulation of the immune checkpoint network and warrant exploitation for therapeutic gains. In lieu of a candidate strategy, the current study integrated bioinformatics analyses with molecular validation to identify cancer-associated miRNAs. Here we report the identification of a miRNA which targets immune checkpoint genes and can be used as a novel tumor biomarker and a therapeutic target in advanced breast cancer.

2. Materials and methods

2.1. Data collection and preparation

The miRNA-seq and RNA-seq data of TCGA BRCA (breast invasive carcinoma) dataset were retrieved from DriverDB [19–21] and YM500 [22–24], and the relevant clinical data were also collected. The experiments validated relations between miRNA and the immune checkpoint genes were based on miRTarbase [25]. The predicted relationship between miRNAs and the immune checkpoint genes were assessed by YM500 and defined by 12 computational tools.

2.2. Differential expression of ICB miRNAs in TCGA BRCA

To perform differential expression analysis of ICB miRNAs, miRNA expressions of 1078 primary tumor samples and 104 adjacent normal samples were included. By using an R package, DEseq [26], differentially expressed miRNAs can be identified with adjusted p-value <0.05 and log₂ fold change <−1. The raw counts of mapped reads for each miRNA were applied to assess the comparisons between and within samples in order to determine the differentially expressed candidates.

2.3. Survival analysis of ICB miRNAs

Survival analysis was performed to investigate the clinical importance of ICB miRNAs by Cox proportional hazards model of each miRNA. Patients were classified into two groups, stratified by the median of miRNA expression. Significant miRNAs associated

with 5-year survival were selected with log-rank p-value <0.05 and hazard ratio <1.

2.4. Cell culture and reagents

The TNBC cell lines of the humans, MDA-MB-231 and BT549, and the mouse, 4T1, were obtained from ATCC. Cells were cultured in DMEM/F12 supplemented by 10% FBS (Hyclone, GE Healthcare Life Sciences) and 1% penicillin/streptomycin (Biological Industries) in a 5% CO₂ incubator at 37°C. hsa-miR-4759 mimics and hsa-miR-scramble controls were purchased (Dharmacon). The lentiviral vectors pCDH and pCDH-PD-L1-WT were provided by Dr. Mien-Chie Hung's Laboratory. Cells were infected with the viral particles derived from pCDH or pCDH-PD-L1-WT followed by selection by puromycin (#101-58-58-2; CyruBio-science). The antibodies of PD-L1 (#GTX104763) and β -actin (#sc-47778) for western blotting were purchased from GeneTex, and Santa Cruz Biotechnology, respectively. ELISA kit for IFN- γ (#EHIFNG) was purchased from Invitrogen, ELISA kits for TNF- α (# KHC3011), IL-10 (#431411), and Granzyme B (#439207) were purchased from BioLegend. The antibodies used for flow cytometry, CD45-FITC (#11-0451-82), CD3 ϵ -PE (#12-0031-82), CD4-PE-Cy7 (#25-0042-82), and CD8-APC (#17-0083-81) (eBioscience). The antibodies used for immunohistochemistry staining, anti-PD-L1 antibody (#17952-1-AP, Proteintech), anti-IFN- γ antibody (ab9657, Abcam), anti-TNF- α antibody (sc-52746, Santa Cruz), and anti-IL-10 antibody (MAB417, R&D). The antibodies were used for PD-L1 blockade in *in vitro* PBMC killing assay and animal experiments, InVivoMab anti-human PD-L1 (#BE0285, BIO X CELL), InVivoMab anti-mouse PD-L1 (#BE0101, BIO X CELL).

2.5. Cell transfection with miRNA mimics

The miR-4759 mimics and the control miR-scramble were transfected into cells using Lipofectamine 2000 (Invitrogen) following the manufacturer's instructions. Protein lysates and total RNA were collected 48 h after the transfection. The expression levels of the miRNAs were verified by qRT-PCR analysis.

2.6. qRT-PCR

Total RNA was isolated using the TRIzol reagent (Life Technologies) following the manufacturer's instructions. cDNAs were synthesized with the MMLV reverse transcription kit (Invitrogen). The expression levels of the miRNAs were analyzed by qRT-PCR [27,28]. The expression of PD-L1 was analyzed using iQ SYBR Green Supermix (Bio-Rad). The fold changes were determined using the comparative cycle threshold method and normalized to β -actin. All experiments were performed in triplicate.

2.7. Luciferase reporter assay

The 3'-UTR regions of PD-L1 containing the miR-4759-binding sites were synthesized (Integrated DNA Technologies). The nucleotide fragments were inserted in the 3'-UTR of the luciferase gene in the pmirGLO Dual-Luciferase vector (Promega). Mutations of the putative miR-4759 3'-UTR were generated using QuikChange Mutagenesis Kit (Agilent Technologies). The luciferase reporter with the miR-4759 mimic or the control miRNA were co-transfected into cells using Lipofectamine 2000. Luciferase activities were measured 48 h after transfection using the luciferase assay kit (Promega).

2.8. *In vitro* PBMC killing assay

Human PBMCs were isolated from the blood from healthy donors and activated with 100 ng/mL anti-CD3, 100 ng/mL anti-CD28, and 10 ng/mL IL2 (#317303; #302913; #589102) (BioLegend), and then co-cultured with tumor cells at 10:1 ratio. Cell death was assessed by a fluorescence caspase-3/7 substrate (#4440, Essen Bioscience) and monitored by the IncuCyte live imaging system (Sartorius).

2.9. Animal models

All animal experiments were conducted following the animal protocols approved by the LAMS of the China Medical University. In the *ex vivo* experiment, 4T1-Luc cells were transfected with miR-4759 or miR-Scr for 24 h. The transfected cells (2.5×10^4) were mixed in 40 μ l PBS/Matrigel (Corning) and injected into the mammary fat pad of 6-week-old female Balb/c or SCID mice ($n = 5$ for each group). Tumor growth was monitored by IVIS (Xenogen). Mice were sacrificed on day 28 to measure the tumor weights and prepare for tissue sections. For intratumoral treatment experiments, 2.5×10^4 4T1-Luc cells in 40 μ l PBS/Matrigel were injected into the mammary fat pad of Balb/c mice (day 0). On day six, the tumors were treated by intratumoral injection of miR-4759 or miR-Scr (every two days at a dose of 1.5 mg/kg) encapsulated with the polymer jetPEI (total injection volume 20 μ l) following the manufacturer's instructions (Polyplus Transfection). Tumor growth was monitored by IVIS (Xenogen). Mice are sacrificed on day 28 to measure tumor weights and prepare for tissue sections.

2.10. Analysis of tumor-infiltrating *t* lymphocyte by flow cytometry

Tumor tissues extracted from mice were washed by serum-free media, minced, and the tissue blocks were disintegrated into single cells by a gentleMACS dissociator (Miltenyi) in PBS buffer containing DNaseI/collagenase. Red blood cells were lysed with the RBC lysis buffer, and the suspended cells were blocked with 5% BSA in PBS and stained with 7-AAD and one of the antibodies CD45-FITC, CD3e-PE, CD4-PE-Cy7, and CD8-APC. Stained samples were analyzed with a FACSVerse cytometer (BD).

2.11. Immunohistochemistry staining

The tissue sections were deparaffinized and hydrated at 65 °C for 1 h followed by 30 min xylene incubation. After washing in a concentration gradient of alcohol for 3 min, antigen retrieval was performed in 1 \times citrate buffer. The endogenous peroxidase activity was blocked with 3% H₂O₂ in methanol for 7 mins. The slides were then washed with TBST or PBS buffer for 10 mins. Endogenous biotin reactivity was blocked with 5% normal goat serum for 1 h. Primary antibodies diluted in 5% normal goat serum were then applied overnight. The primary antibodies were removed by washing with TBST or PBS buffer for 15 mins. Secondary antibodies diluted in 2.5% normal goat serum were then applied for 1 h. After washing with TBST for 15 mins, avidin–biotin complex (ABC) was applied to the slides and incubated for 1 h followed by washing with TBST for 15 mins. The staining was visualized by the DAB reaction and counter-stained by hematoxylin.

2.12. *In situ* hybridization

The detection probes including miR-4759 targeted probe and U6 snRNA control probe conjugated with DIG, and buffer set were purchased from Qiagen. The ISH was performed in manufacturer's instruction. Briefly, the tissue sections were deparaffinized at 65°C

for 1 h followed by 30 min xylene incubation, rehydrated in concentration gradient ethanol and washed in ddH₂O and PBS. Proteinase K Incubation at 37°C for 10 min and wash twice in PBS. Tissue sections were hybridized with 40nM targeted and 1nM control probes at 55°C for 1 h. Wash the tissue section in concentration gradient SSC buffers. Blocking was performed in blocking buffer at RT for 15 min and tissue sections were incubated with anti-DIG at RT for 1 h. Wash with PBS and incubate with AP substrate for signal development at 30°C for 1.5 h. KTBT buffer was employed to stop the reaction. Counter staining was performed in Nuclear Fast Red.

2.12. Statistical analysis

All statistical analyses were performed using EXCEL 2019. The results were reported as mean \pm standard deviation. Statistical analyses were conducted using Student's *t*-test and Pearson Correlation Coefficient. $P < 0.05$ was considered statistically significant.

3. Results

3.1. Systematic identification of ICB miRNAs through an integrated bioinformatics strategy

Twenty seven genes encoding important inhibitory checkpoint proteins were selected based on literature annotation (Supplementary Table S1) [29–55], and the candidate miRNAs regulating these genes were predicted by an *in silico* approach using an integrated bioinformatics strategy (Fig. 1A). Firstly, to identify the relationships between the inhibitory checkpoint genes and miRNAs, a curated database of experimentally validated miRNA–gene interactions (miRTarbase) was queried. In addition, 12 miRNA prediction tools for potential miRNA–target gene interactions were employed to cross-interrogate for potential miRNAs involved in the regulation of the selected target checkpoint genes. This initial drive identified 713 miRNA candidates based on the validated miRTarbase database and the predicted interactions suggested by at least six prediction tools. Next, we reasoned that expression of the checkpoint-suppressing miRNAs should be downregulated in tumor tissues compared to the normal tissue counterparts. Thus, an analysis for differential expression of the 713 miRNAs between primary tumors and the adjacent normal tissues of patients with breast cancer in the TCGA datasets was carried out. The analysis predicted 41 miRNAs whose expression was preferentially downregulated in primary tumors (Fig. 1B). These 41 miRNAs were further tested for association with patient survival. Among them, two stood out with a significant correlation with favorable survival prognosis (Fig. 1C). One of the two miRNAs, miR-4759, was negatively correlated with its predicted target, the immune checkpoint gene PD-L1, in gene expression. PD-L1 is the sole target gene predicted by more than 6 prediction tools to be downregulated by miR-4759 based on the selection workflow (Fig. 1, A and D). Consistently, the negative expression correlation of miR-4759 and PD-L1 was supported by Spearman's rank-order correlation analysis (Fig. 1E). DE analysis showed the expression of miR-4759 was significantly lower in tumor tissues of breast cancer than the normal tissues (Fig. 1F). Moreover, analyzing miR-4759 expression in each breast cancer subtype of the TCGA dataset (Supplementary Table S2), we found that the luminal-like subtypes (luminal A and luminal B) had higher expression significantly than the triple-negative subtype (Fig. 1G). Furthermore, Kaplan–Meier analysis illustrated a significant association of high miR-4759 expression with better 5-year survival in breast cancer patients (Fig. 1H). To fully characterize the tumor microenvironment in the context of miR-4759 expression in human breast cancer, the

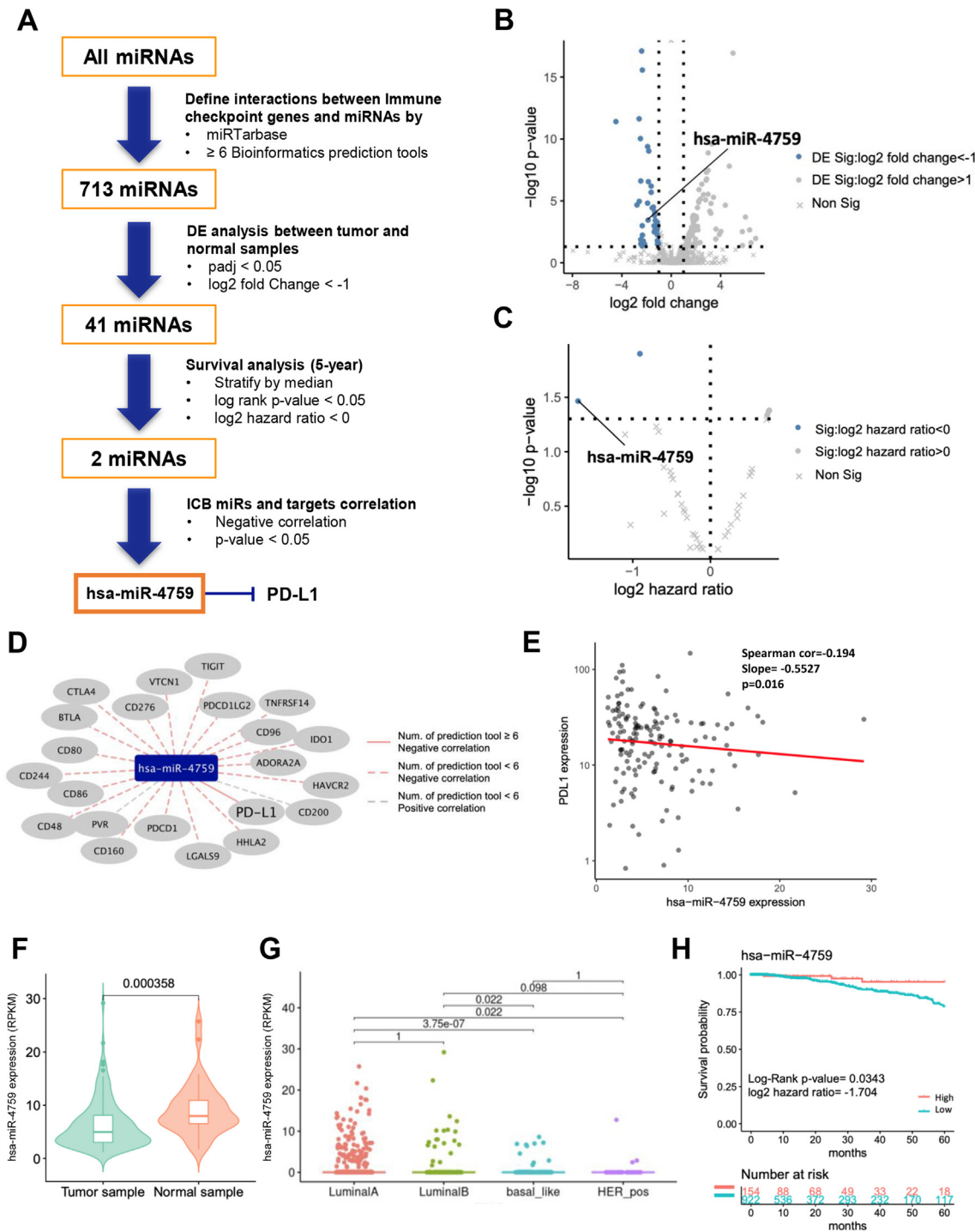


Fig. 1. Identification of miRNAs suppressing immune checkpoint genes. (A) The workflow of identifying miRNAs targeting immune checkpoint genes which were selected based on literature annotation. Candidate miRNAs with a potential of targeting these immune checkpoint genes were then panned through multiple measures first by the predicted interactions with the tested immune checkpoint genes, followed by their differential expression in cancer versus normal tissues, the correlation between the expression of the miRNAs and the predicted target genes, and the association with patient survival. The panning process resulted in the identification of only one miRNA, hsa-miR-4759. (B) The scatterplot of statistical significance (p-value) versus differential expression (DE) of the miRNAs in tumors and normal tissues by the volcano plot. The values of the x-axis are log2 transformation of fold changes (log2 Fold Changes) of expression, and the values of the y-axis are negative log10 transformation of p-values ($-\log_{10}$ p-values) estimated by DEseq. (C) The scatterplot of p-values versus hazard ratios of the miRNAs in patients with breast cancer was demonstrated by the volcano plot. The values of the x-axis are log2 transformation of hazard ratios, and the values of the y-axis are $-\log_{10}$ p-values estimated by log-rank test. (D) The network showed the relationship between hsa-miR-4759 and the predicted cognate targets. The expression correlation between the miRNAs and their targets was calculated using Spearman's rank-order correlation. (E) The expression of miR-4759 was negatively correlated with its target gene PD-L1 (coefficient value -0.194). (F) DE analysis showed that miR-4759 was significantly down-regulated in tumor sites compared to normal tissues in patients with breast cancer. (G) DE analysis showed that miR-4759 was significantly down-regulated in HER2-positive and basal-like breast cancers compared to luminal A breast cancers in TCGA BRCA dataset. (H) Kaplan-Meier analysis illustrated that low expression of hsa-miR-4759 was significantly associated with poor overall survival.

correlations of miR-4759 expression between a group of 298 genes including immune checkpoints, cytokine signaling, and tumor inflammation were analyzed. Among them, PVR, CD80, CCL7, CCL8, and STAT1 were found inversely correlated with miR-4759 expression (Supplementary Table S3). These genes have been reported to play major roles in the immunosuppression during tumor progression: PVR plays a critical role in suppressing the anti-tumor effects of cytotoxic T cells and NK cells by binding with TIGIT [39,40], CD80-CTLA-4 axis inhibits proliferation of CD8 T cells and causes immune tolerance in cancer progression [30,46], STAT1 overexpression and activation causes PD-L1 upregulation and MDSC infiltration in the tumor microenvironment [56], CCL7 and CCL8 are well-known chemokines secreted from MDSCs to that increase resistance of ICB therapy [57,58]. Together, these results suggest that miR-4759 is a potential immune checkpoint blocker by targeting the PD-L1 gene in breast cancer cells.

3.2. PD-L1 is a direct target of miR-4759

Sequence analysis unveiled two putative binding motifs of miR-4759 in the 3'-UTR of the PD-L1 gene (Fig. 2A, designated as site 1 and site 2). To test their function in gene regulation, reporter constructs were constructed in which the DNA motifs containing the putative miR-4759-binding sites of the wild-type or mutated sequence were cloned in the 3' end of a luciferase reporter gene (Fig. 2A). Transduction of miR-4759 inhibited luciferase activity derived from the construct with wild-type but not the mutant miR-4759-binding motif in two human TNBC cell lines MDA-MB-231 and BT549 (Fig. 2, B and C). Moreover, miR-4759 overexpression significantly inhibited the reporter activity derived from the construct with wild-type site 1 but mutated site 2 compared to the reporter with mutated site 1 but wild-type site 2, suggesting site 1 (position 1950–1957) the major miR-4759-binding motif (Fig. 2D). Furthermore, ectopic expression of miR-4759 significantly down-regulated PD-L1 expression as demonstrated by quantitative real-time PCR (qRT-PCR) of mRNA levels (Fig. 2E) as well as by Western blotting analyses of protein levels (Fig. 2F) in both TNBC cell lines. Taken together, these findings suggest that miR-4759 directly binds to the 3'-UTR motifs of the PD-L1 gene and suppressed PD-L1 expression.

3.3. miR-4759 enhances the sensitivity to PBMC-mediated cytotoxicity via PD-L1 down-regulation

Upregulation of PD-L1 expression in cancer cells is one of the major causes of evading anti-tumor immunity. Thus, we speculated that the expression of miR-4759 should enhance the sensitivity of TNBC cells to T cell immunity. To test this hypothesis, TNBC cells were co-cultured with peripheral blood mononuclear cells (PBMC) in a cell-killing assay. As expected, transduction of miR-4759 mimics efficiently sensitizes the MDA-MB-231 and BT549 to killing by PBMC (Fig. 3, A and B). Furthermore, TNBC cells transfected with miR-4759 mimics significantly increased secretion of IFN- γ , TNF- α as well as granzyme B, and decreased IL-10 into the culture media with co-cultured PBMC (Fig. 3C). MTT assay demonstrated that transduction of miR-4759 alone did not affect cell viability of TNBC cells (Supplementary Fig. S1), indicating an underlying mechanism of PBMC-mediated immunity of miR-4759-mediated cell death. To determine that the immune-sensitizing effect by miR-4759 required the down-regulation of the endogenous PD-L1, PD-L1 expression was reconstituted with a PD-L1 cDNA construct lacking the 3'-UTR, hence was resistant to miR-4759-mediated repression, in TNBC cells. The ectopic PD-L1 was expressed despite the presence of miR-4759 as shown by Western blotting analysis (Fig. 3D), resulting in desensitization of TNBC cells to PBMC-mediated killing in MDA-MB-231 and BT549

cells (Fig. 3, E and F). In vitro cell killing assays showed that transduction of miR-4759 mimics promoted PBMC-mediated cytotoxicity to similar levels by the treatments with the anti-PD-L1 antibody alone or miR-4759 plus anti-PD-L1 (Fig. 3, G and H). Taken together, these results demonstrated that miR-4759 repressed PD-L1 expression in cancer cells thus promoting anti-tumor immunity.

3.4. miR-4759 increased tumor-infiltrating lymphocytes and suppressed tumor growth in vivo in a syngeneic mouse model

To our knowledge, the potential murine miR-4759 homolog has not been reported. To address this issue, we performed a stem-loop PCR on RNA isolated from the murine TNBC cell line 4T1 and successfully amplified a potential human miR-4759 homolog. Direct sequencing showed that it is identical to the human miR-4759 (Supplementary Fig. S2). We then set out to test the potential function of miR-4759 in immune rejection using an immunocompetent murine system. 4T1 cells stably expressing luciferase (4T1-Luc) were transfected with miR-4759 and transplanted into the syngeneic BALB/c mice as well as the immune-deficient SCID mice (Fig. 4A). Tumors derived from miR-4759-expressing 4T1 cells grew significantly slower than tumors derived from control cells transfected by control miRNA of scrambled sequence (miR-Scr) in BALB/c mice. Conversely, no significant difference in tumor growth was observed in SCID mice, suggesting that immune competency is required for the anti-tumor effect of miR-4759. In direct corroboration, tumors treated with miR-4759 grew slower than the tumors of the control group (Fig. 4, B and C). Indeed, immunohistochemical staining showed that expression of PD-L1 in miR-4759-treated tumors was significantly lower than the control group (Fig. 4D), accompanied by increased tumor-infiltrating CD8⁺ T lymphocytes (TIL) in 4T1-Luc tumors as scored by flow cytometry. Treatment with miR-4759 indeed significantly increased TIL presentation in mice (Fig. 4E). Moreover, immunohistochemical staining also showed increased secretion of IFN- γ as well as TNF- α , and decreased IL-10 in miR-4759-treated tumors than the control group, suggesting that miR-4759 supported the formation of an activated immune microenvironment in breast tumors (Fig. 4F). To further assess the cytotoxicity efficacy of miR-4759, systemic miR-4759 treatment combined with paclitaxel was compared to the FDA-approved first-line therapy of anti-PD-L1 combined with paclitaxel in syngeneic 4T1 tumor-bearing mouse model. The data show that miR-4759 combined with paclitaxel was more efficient in tumor suppression than anti-PD-L1 combined with paclitaxel (Supplementary Fig. S3). As documented by prior studies [59], prolonged treatment with the anti-PD-L1 antibody resulted in significant death of the treated mice, preventing the pursuing of a longer treatment course (data not shown). These data suggested that miR-4759 down-regulated PD-L1 expression and increased CD8⁺ T cell infiltration in tumor tissues to suppress tumor growth.

3.5. miR-4759 is inversely correlated with PD-L1 expression in human breast tumors

The results presented above would predict a reverse correlation between the expression of miR-4759 and PD-L1 in human breast cancer tumors tissues. To test this hypothesis, expression of miR-4759 was assessed by *in situ* hybridization (ISH) and PD-L1 expression was examined by IHC staining in the tumor tissues of a cohort of breast cancer patients (n = 181) (Fig. 5A, Supplementary Table S4). Analysis of average H-scores showed that PD-L1 expression is significantly higher in tumors with relatively lower expression of miR-4759, and *vice versa* (Fig. 5B). The result supports a reverse correlation between PD-L1 and miR-4759 and is consistent

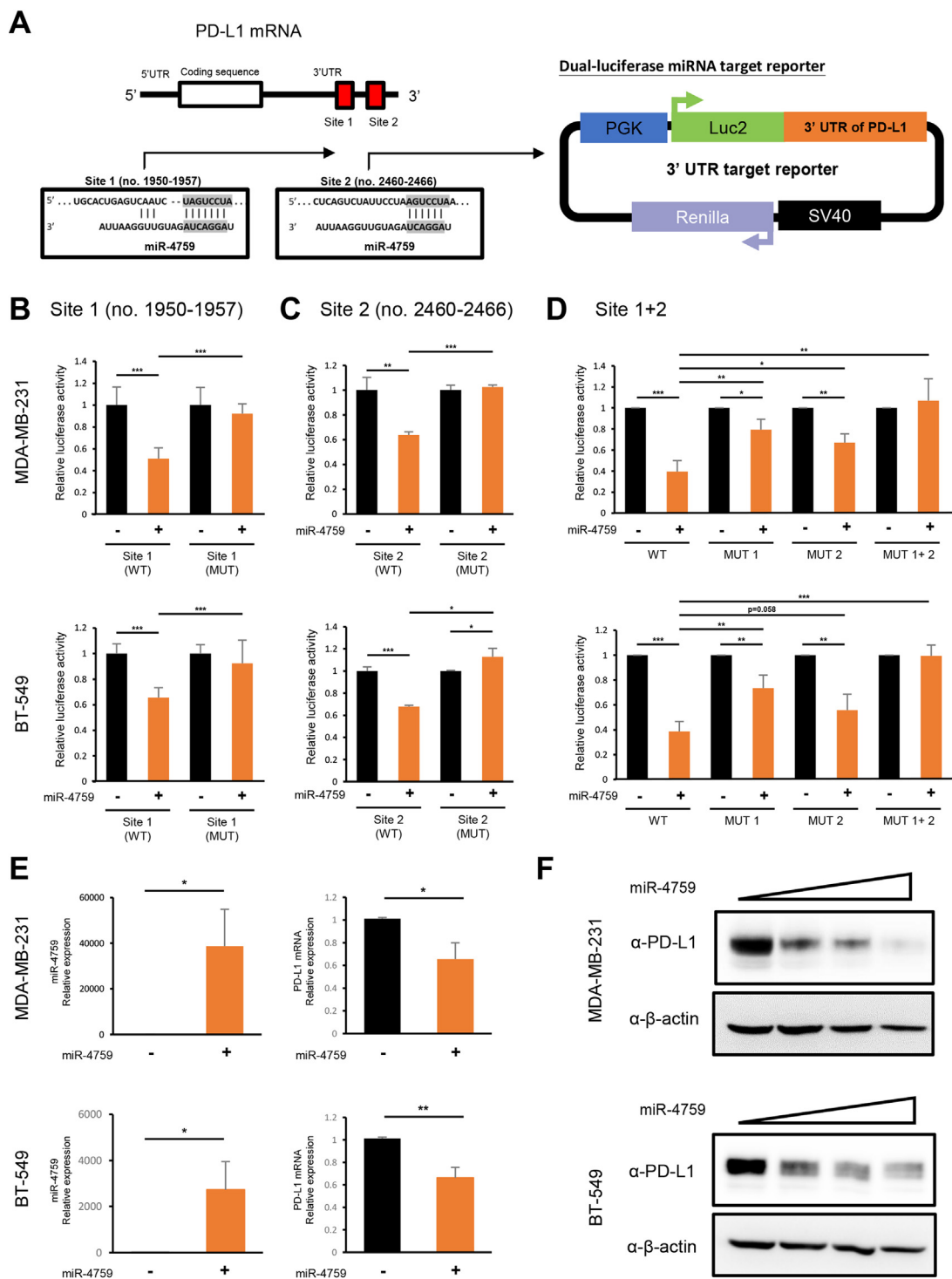


Fig. 2. PD-L1 is directly repressed by miR-4759. (A) PD-L1 is a potential target of miR-4759. Predicted target sequences for miR-4759 human PD-L1 mRNA are shown. (B, C, D) The luciferase vectors that contain the human wild-type (WT) and mutant (MUT) targeting sites of PD-L1 3'-UTR regions were co-transfected into MDA-MB-231 and BT-549 cells with miR-4759 or scramble miRNA (miR-Scr). The relative luciferase/Renilla activities were analysed in the cells 48 h after the transfection. The results represent the mean \pm SD. from six independent experiments. Statistical significance was tested by *t*-test. *, $p < 0.05$; **, $p < 0.01$; ***, $p < 0.001$. (E) MDA-MB-231 and BT-549 cells were transfected with miR-4759 or miR-Scr. miR-4759 and PD-L1 mRNA levels were determined via qRT-PCR assay. Statistical significance was tested by *t*-test. *, $p < 0.05$; **, $p < 0.01$. The results represent the mean \pm SD. from three independent experiments. (F) MDA-MB-231 and BT-549 cells were transfected with miR-4759 or miR-Scr. The expression levels of PD-L1 were analysed by western blotting. One representative experiment of three experiments is shown.

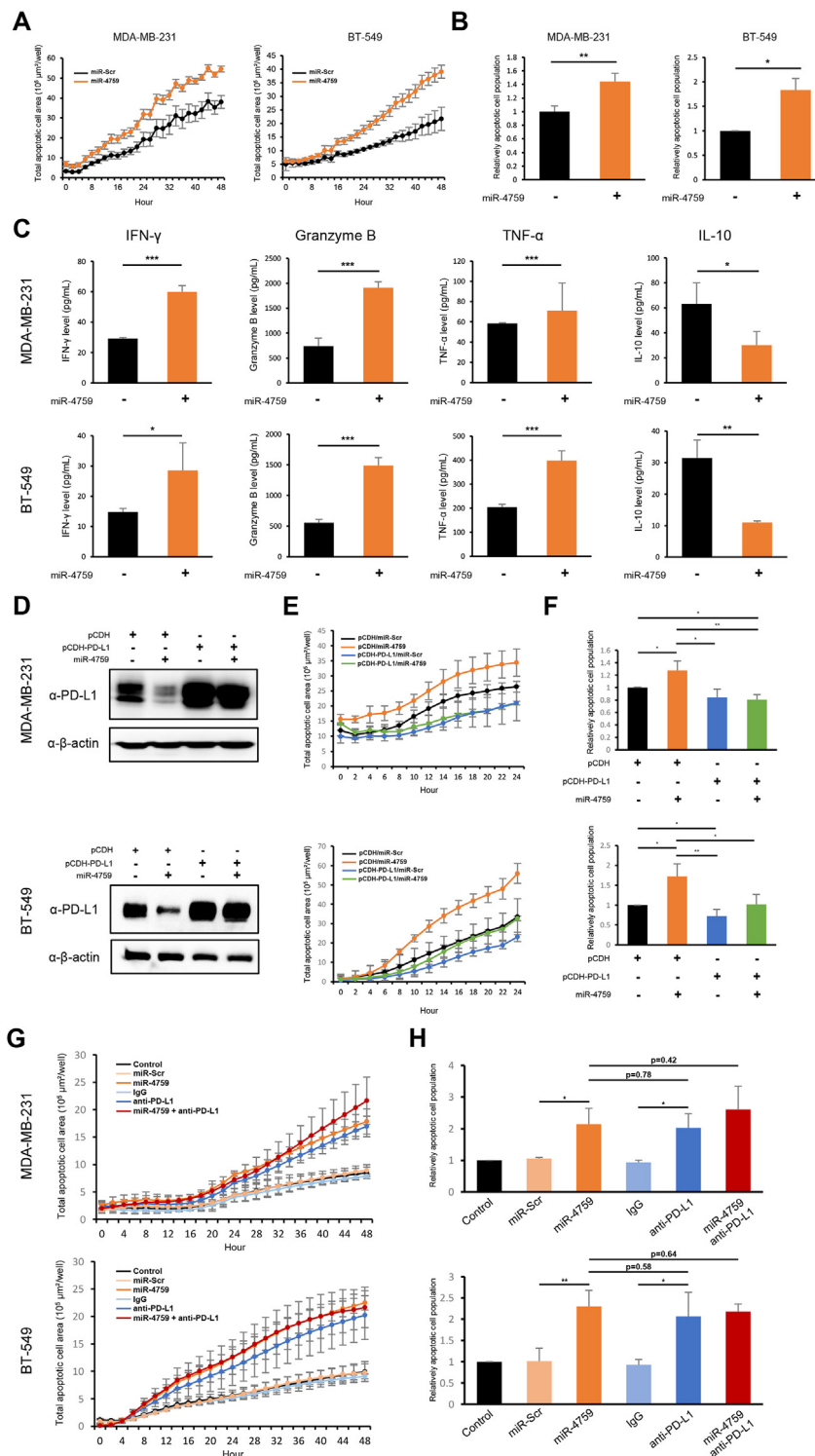


Fig. 3. miR-4759 enhances the cytotoxicity of PBMCs to TNBC cells via PD-L1 down-regulation in co-culture model. (A) MDA-MB-231 and BT-549 cells were transfected with miR-4759 or miR-Scr. PBMCs were subsequently co-cultured with miR-treated TNBC cells in IncuCyte for 48 h. The apoptotic cell population was determined with green fluorescent signals. (B) The relative apoptotic population of miR-4759 treated cells was compared with miR-Scr group. The results represent the mean ± SD. from three independent experiments. Statistical significance was tested by *t*-test. *, *p* < 0.05. (C) Co-culture media were assayed for IFN- γ , Granzyme B, TNF- α and IL-10 by cytokine ELISA assay. The results represent the mean ± SD. from three independent experiments. Statistical significance was tested by *t*-test. *, *p* < 0.05; **, *p* < 0.01; ***, *p* < 0.001. (D) TNBC cells with or without stable overexpression of PD-L1 were transfected with miR-4759 or miR-Scr. The expression levels of PD-L1 were analysed by western blotting. One representative experiment of three experiments is shown. (E) TNBC cells with or without stable overexpression of PD-L1 were transfected with miR-4759 or miR-Scr. PBMCs were subsequently co-cultured with miR-treated TNBC cells in IncuCyte for 24 h. Apoptotic cells were determined with green fluorescent signals. (F) The relative apoptotic population of miR-4759 treated cells was compared with miR-Scr group. The results represent the mean ± SD. from three independent experiments. Statistical significance was tested by *t*-test. *, *p* < 0.05, **, *p* < 0.01. (G) MDA-MB-231 and BT-549 cells were transfected with miR-4759/miR-Scr or treated with control IgG/anti-PD-L1. PBMCs were subsequently co-cultured with treated TNBC cells in IncuCyte for 48 h. The apoptotic cell population was determined with green fluorescent signals. (H) The relative apoptotic population of different groups was compared with the control group. The results represent the mean ± SD. from three independent experiments. Statistical significance was tested by *t*-test. *, *p* < 0.05, **, *p* < 0.01. (For interpretation of the references to colour in this figure legend, the reader is referred to the web version of this article.)

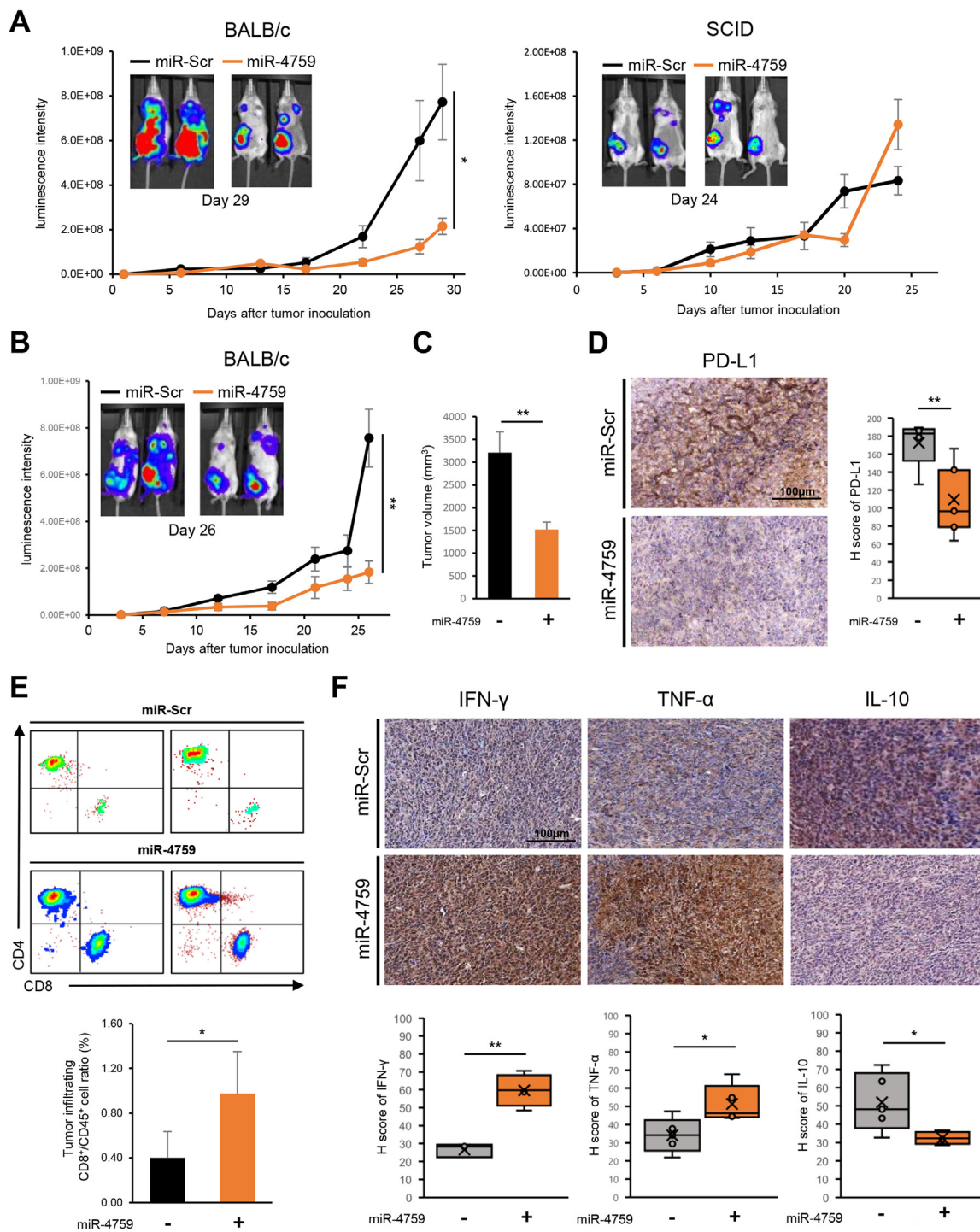


Fig. 4. miR-4759 intratumoral treatment suppresses tumor growth, correlated with less PD-L1 expression and more infiltrating CD8 cells in 4T1 tumors. (A) Tumor growth of 4T1 cells transfected with miR-4759 or miR-Scr in BALB/c or BALB/c SCID mice. n = 5 mice per group. Statistical significance was tested by *t*-test. *, *p* < 0.05. (B) Tumor growth of 4T1 cells in BALB/c mice treated with miR-4759 or miR-Scr intratumorally. n = 5 mice per group. Statistical significance was tested by *t*-test. **, *p* < 0.01. (C) Tumors were excised, and tumor volume was measured on day 27 from mice treated with miR-4759 or miR-Scr intratumorally. The arrow mark indicates the day start treatment. n = 5 mice per group. Statistical significance was tested by *t*-test. **, *p* < 0.01. (D) Representative images of PD-L1 IHC-staining of tumor tissues harvested from mice treated with miR-4759 or miR-Scr intratumorally. PD-L1 was measured by H-score. n = 5 mice per group. Statistical significance was tested by *t*-test. *, *p* < 0.05. (E) Quantification of tumor-infiltrating CD8⁺ T cell populations in mice treated with miR-4759 or miR-Scr intratumorally. n = 5 mice per group. Statistical significance was tested by *t*-test. *, *p* < 0.05. (F) Representative images of IFN- γ , TNF- α , and IL-10 IHC-staining of tumor tissues were harvested from mice treated with miR-4759 or miR-Scr intratumorally. Protein levels were measured by H-score. Statistical significance was tested by *t*-test. *, *p* < 0.05, **, *p* < 0.01.

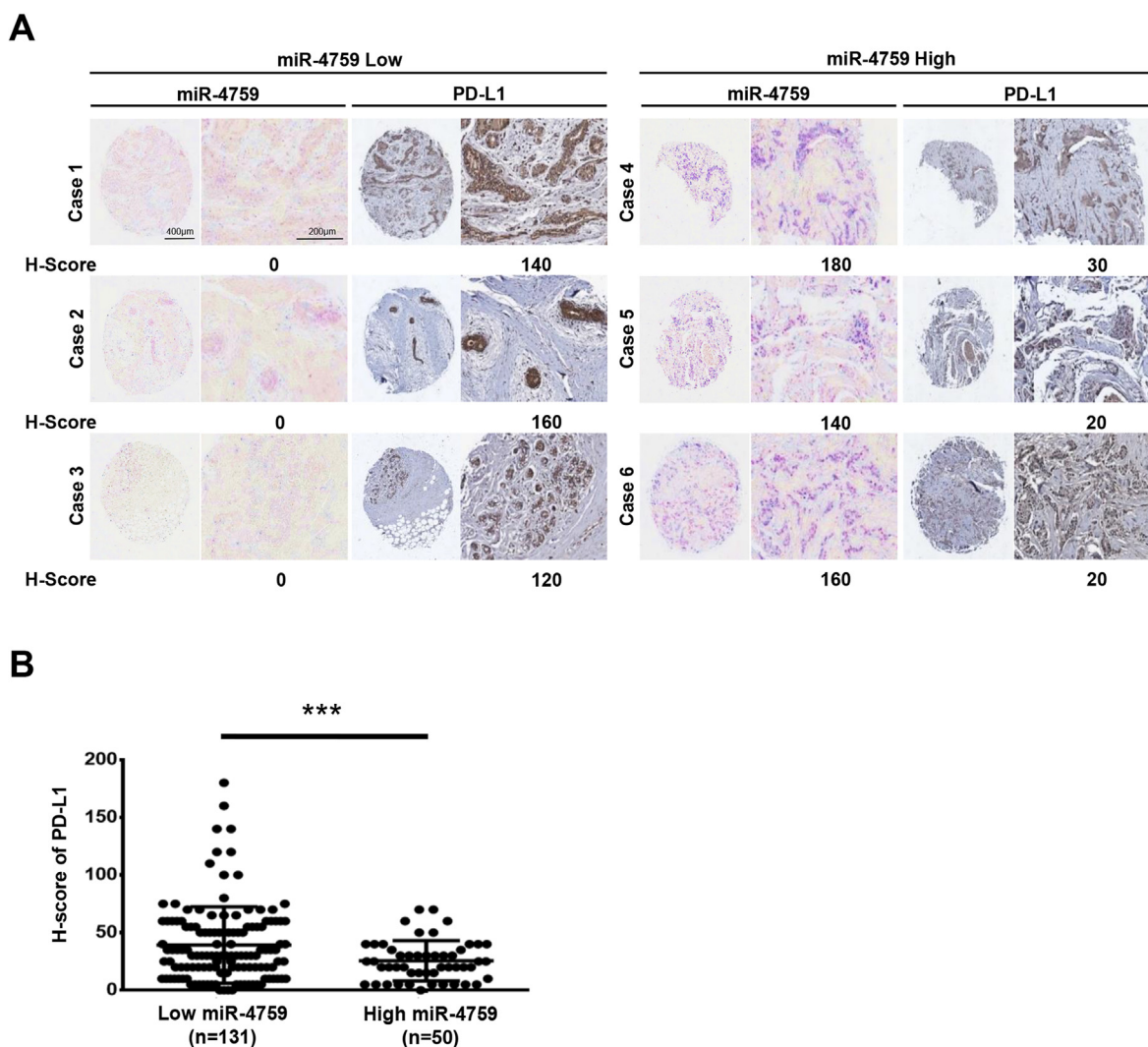


Fig. 5. miR-4759 is inversely correlated with PD-L1 expression in human breast tumors. (A) Representative ISH images of miR-4759 and IHC images of PD-L1 in 181 breast cancer specimens. (B) IHC staining of PD-L1 was scored and the data were plotted. PD-L1 expressions were compared between low miR-4759 level and high miR-4759 level (separated by average value), Bars, mean (the middle bar), and the standard deviation (the upper and lower bars). Statistical significance was tested by an unpaired *t*-test. ***, *p* < 0.001.

with the finding that miR-4759 repressed PD-L1 expression in breast cancer.

4. Discussion

To rationally identify miRNAs targeting immune checkpoint genes, we have developed an integrative bioinformatics approach entailing four strategies: miRNA-gene identification leveraging a validated miRNA database and a comprehensive cohort of 12 predictive tools, differential expression analysis, correlation with patient outcome, and expression correlation between the candidate miRNAs and the predicted target. This strategy offers the uniqueness of our study among others of the kind in systematically interrogating the miRNA-immune checkpoint networks. Utilizing this strategy, we have discovered that miR-4759 is bound to the 3'-UTR of the PD-L1 gene in a sequence-specific manner and repressed PD-L1 expression in breast cancer. Corroborating to this discovery, the expression of the human miR-4759 was inversely correlated with PD-L1 expression in breast tumors. As PD-L1 expression is known for its function in immune suppression, knowledge of the causal factors of PD-L1 regulation besides inter-

ferons is highly demanded. Those results proved the feasibility of the bioinformatics strategy and provided insight into investigating miRNA-gene networks related to the immune checkpoint mechanism.

PD-L1 expression is known to be subject to regulation by miRNAs [60]. It has been reported that the tumor suppressor p53 can inhibit the expression of PD-L1 by transactivating the expression of the miR-34 family members miR-34a, miR-34b, and miR-34c which in turn down-regulate PD-L1 by binding to its 3'-UTR in non-small cell lung cancer [61]. Also in lung cancer, it has been demonstrated that miR-200 represses the expression of PD-L1 by targeting the 3'-UTR of the gene [62]. However, the expression of these miRNAs was not correlated with tumor development in patients with breast cancer. In comparison with these miRNAs, miR-4759 is a relatively novel miRNA of which the function in suppressing immune checkpoint has not been identified. Furthermore, unlike other miRNAs, the tumor suppression function of miR-4759 was identified in cellular contexts in BT-549 and MDA-MB-231 with a deficiency of p53. Our study for the first time demonstrated that miR-4759 is an evolutionarily conserved immune-sensitizing non-coding RNA.

Secretion of the cytokine IFN- γ and granzyme B from both BT-549 and MDA-MB-231 cell lines co-incubated with PBMC was induced by treatment with miR-4759. TNF- α secretion, on the other hand, was induced from the PBMC co-culture of BT-549 but not MDA-MB-231. The mechanisms underlying the differential release of TNF α are not clear but it is conceivable that cell context-dependent regulation of immune response may be involved. More importantly, the tumor suppression activity of miR-4759 was observed in the immunocompetent milieu and not in the immunodeficient environment, supporting the involvement of immune cells in the tumor-suppressing activity of miR-4759. As a proof of concept, we showed that intratumoral injection of miR-4759 suppressed tumor progression and metastasis, suggesting that the miRNA is a promising strategy in therapeutic application.

Treatment with monoclonal antibodies recognizing the extracellular domain of the membrane-bound PD-1 and PD-L1 as immune checkpoint inhibitors have been increasingly employed for cancer therapy. Expression of PD-1 and PD-L1 in tumor tissues is a stratification marker predicting responsiveness to ICB treatments [63,64]. In spite of high enthusiasm, responsiveness to the treatments has not been superior for breast cancer and other cancer types at advanced stages [65]. The mechanisms of resistance to the anti-PD-1/PD-L1 treatments are complex. Recent studies demonstrated that tyrosine phosphorylation and glycosylation of the cell surface PD-L1 play a key role in promoting the protein stability and immune-suppressing function of PD-L1 [9,66–68]. It is noteworthy that glycosylated PD-L1 can also be shielded from immunohistochemical detection thus hindering accurate assessment of the expression status of the immune checkpoint protein in tumor tissues [10]. Furthermore, besides the traditional immunosuppression function through PD-1 interaction, intracellular PD-L1 that is spared from the attack of therapeutic antibodies has been shown to participate in DNA damage repair and foster resistance to chemotherapy [69]. Thus, suppressing gene expression of PD-L1 by molecular strategies such as miRNAs offers a complementary dimension conferring a unique advantage of eradicating the pro-tumor functions regulated by the PD-1/PD-L1 axis and can be extended to other immune checkpoint pathways.

With the advent of small RNA drugs and mRNA vaccines in clinical applications, RNA-based therapy offers an exciting opportunity to expand the range of therapeutic targets. Our results suggest that administration of miR-4759 through local injection or systematically transduced by nanoparticles can be a promising treatment option for patients whose tumors are PD-L1-positive, and therefore immunorepressive, but do not respond to the conventional anti-PD-1/PD-L1 antibodies. Furthermore, the combination of miR-4759 with other immune checkpoint inhibitors may reinforce the anti-cancer immunity of patients with breast cancer.

Acknowledgements

The authors thank Yu Hung for helping edit and proofreading the manuscript. This study was supported in part by the Research Center for Cancer Biology of the China Medical University and the Center for Molecular Medicine of the China Medical University Hospital. Experiments and data analysis were performed in part through the use of the Medical Research Core Facilities Center, Office of Research & Development at China Medical University, Taichung, Taiwan.

Author contributions

S.-C.W. and W.-C.C. conceived the project, designed the experiments, coordinated the collaborating groups, and prepared the manuscript. Y.-Z.L. performed most of the experiments,

contributed manuscript preparation, and coordinated working sub-groups. S.-H.L. contributed to bioinformatics analysis and manuscript preparation. Y.-L.W. and Y.-Z.L. generated reporter constructions. Y.-Z.L., W.-R.W., C.-C.L. and P.-L.L. conducted animal experiments. Y.-L.W. and Y.-C.S. conducted IHC and FISH experiments. L.-C.L. and H.C. contributed to human tumor tissue acquisition, analysis and pathological assessments.

Conflict of interest

A patent application has been submitted to Intellectual Property Office, Ministry of Economic Affairs, R.O.C. (Taiwan). Shao-Chun Wang, Wei-Chung Cheng, You-Zhe Lin, Shu-Hsuan Liu and Wan-Rong Wu are co-inventors.

Appendix A. Supplementary data

Supplementary data to this article can be found online at <https://doi.org/10.1016/j.csbj.2021.12.020>.

References

- [1] Bray F, Ferlay J, Soerjomataram I, Siegel RL, Torre LA, Jemal A. Global cancer statistics 2018: GLOBOCAN estimates of incidence and mortality worldwide for 36 cancers in 185 countries. *CA Cancer J Clin* 2018;68:394–424.
- [2] Kroemer G, Senovilla L, Galluzzi L, André F, Zitvogel L. Natural and therapy-induced immunosurveillance in breast cancer. *Nat Med* 2015;21:1128–38.
- [3] Pardoll DM. The blockade of immune checkpoints in cancer immunotherapy. *Nat Rev Cancer* 2012;12:252–64.
- [4] He X, Xu C. Immune checkpoint signaling and cancer immunotherapy. *Cell Res* 2020;30:660–9.
- [5] Wykes MN, Lewin SR. Immune checkpoint blockade in infectious diseases. *Nat Rev Immunol* 2018;18:91–104.
- [6] Ribas A, Wolchok JD. Cancer immunotherapy using checkpoint blockade. *Science* 2018;359:1350–5.
- [7] Jonathan M, Vétizou RD, Maríá T, Yamazaki B, Routy PL, Ivo M, et al. Resistance Mechanisms to Immune-Checkpoint Blockade in Cancer 2016;44:1255–69.
- [8] Curdy N, Lanvin O, Laurent C, Fournié J-J, Franchini D-M. Regulatory Mechanisms of Inhibitory Immune Checkpoint Receptors Expression. *Trends Cell Biol* 2019;29:777–90.
- [9] Hsu J-M, Xia W, Hsu Y-H, Chan L-C, Yu W-H, Cha J-H, et al. STT3-dependent PD-L1 accumulation on cancer stem cells promotes immune evasion. *Nat Commun* 2018;9.
- [10] Li C-W, Lim S-O, Chung EM, Kim Y-S, Park AH, Yao J, et al. Eradication of triple-negative breast cancer cells by targeting glycosylated PD-L1. *Cancer Cell* 2018;33:187–201.e110.
- [11] Okada M, Chikuma S, Kondo T, Hibino S, Machiyama H, Yokosuka T, et al. Blockage of core fucosylation reduces cell-surface expression of PD-1 and promotes anti-tumor immune responses of T cells. *Cell Reports* 2017;20:1017–28.
- [12] Meng X, Liu X, Guo X, Jiang S, Chen T, Hu Z, et al. FBXO38 mediates PD-1 ubiquitination and regulates anti-tumour immunity of T cells. *Nature* 2018;564:130–5.
- [13] Xie M, Ma L, Xu T, Pan Y, Wang Q, Wei Y, et al. Potential regulatory roles of microRNAs and long noncoding RNAs in anticancer therapies. *Mol Ther Nucleic Acids* 2018;13:233–43.
- [14] Croce CM, Calin GA. miRNAs, cancer, and stem cell division. *Cell* 2005;122:6–7.
- [15] Jan B, Salaun YJ, Douglas G, Merck E, Boudousquie C, Daniel T, et al. MicroRNA-155 is required for effector CD8+ T cell responses to virus infection and cancer. *Immunity* 2013;38:742–53.
- [16] Zhang Y, Sun E, Li X, Zhang M, Tang Z, He L, et al. miR-155 contributes to Df1-induced asthma by increasing the proliferative response of Th cells via CTLA-4 downregulation. *Cell Immunol* 2017;314:1–9.
- [17] Wei J, Nduom EK, Kong L-Y, Hashimoto Y, Xu S, Gabrusiewicz K, et al. MiR-138 exerts anti-glioma efficacy by targeting immune checkpoints. *Neuro-Oncology* 2016;18:639–48.
- [18] Yang J, Liu R, Deng Y, Qian J, Lu Z, Wang Y, et al. MiR-15a/16 deficiency enhances anti-tumor immunity of glioma-infiltrating CD8+ T cells through targeting mTOR. *Int J Cancer* 2017;141:2082–92.
- [19] Liu S-H, Shen P-C, Chen C-Y, Hsu A-N, Cho Y-C, Lai Y-L, et al. DriverDBv3: a multi-omics database for cancer driver gene research. *Nucleic Acids Res* 2019.
- [20] Chung IF, Chen C-Y, Su S-C, Li C-Y, Wu K-J, Wang H-W, et al. DriverDBv2: a database for human cancer driver gene research. *Nucleic Acids Res* 2016;44:D975–9.
- [21] Cheng W-C, Chung IF, Chen C-Y, Sun H-J, Fen J-J, Tang W-C, et al. DriverDB: an exome sequencing database for cancer driver gene identification. *Nucleic Acids Res* 2014;42:D1048–54.

- [22] Chung IF, Chang S-J, Chen C-Y, Liu S-H, Li C-Y, Chan C-H, et al. YM500v3: a database for small RNA sequencing in human cancer research. *Nucleic Acids Res* 2017;45:D925–31.
- [23] Cheng W-C, Chung IF, Tsai C-F, Huang T-S, Chen C-Y, Wang S-C, et al. YM500v2: a small RNA sequencing (smRNA-seq) database for human cancer miRNome research. *Nucleic Acids Res* 2015;43:D862–7.
- [24] Cheng WC, Chung IF, Huang TS, Chang ST, Sun HJ, Tsai CF, et al. YM500: a small RNA sequencing (smRNA-seq) database for microRNA research. *Nucleic Acids Res* 2013;41:D285–94.
- [25] Huang H-Y, Lin Y-C-D, Li J, Huang K-Y, Shrestha S, Hong H-C, et al. miRTarBase 2020: updates to the experimentally validated microRNA–target interaction database. *Nucleic Acids Res* 2019.
- [26] Anders S, Huber W. Differential expression analysis for sequence count data. *Genome Biol* 2010;11:R106.
- [27] Varkonyi-Gasic E, Wu R, Wood M, Walton EF, Hellens RP. Protocol: a highly sensitive RT-PCR method for detection and quantification of microRNAs. *Plant Methods* 2007;3:12.
- [28] Czimmerer Z, Hulvely J, Simandi Z, Varallyay E, Havelda Z, Szabo E, et al. A versatile method to design stem-loop primer-based quantitative PCR assays for detecting small regulatory RNA molecules. *PLoS ONE* 2013;8:e55168.
- [29] Zheng Y, Manzotti CN, Liu M, Burke F, Mead KI, Sansom DM. CD86 and CD80 differentially modulate the suppressive function of human regulatory T cells. *J Immunol* 2004;172:2778–84.
- [30] Nolan A, Kobayashi H, Naveed B, Kelly A, Hoshino Y, Hoshino S, et al. Differential role for CD80 and CD86 in the regulation of the innate immune response in murine polymicrobial sepsis. *PLoS ONE* 2009;4:e6600.
- [31] Ohue Y, Nishikawa H. Regulatory T (Treg) cells in cancer: Can Treg cells be a new therapeutic target? *Cancer Sci* 2019;110:2080–9.
- [32] Janakiram M, Chinai JM, Zhao A, Sparano JA, Zang X. HHLA2 and TMIGD2: new immunotherapeutic targets of the B7 and CD28 families. *Onc Immunology* 2015;4:e1026534.
- [33] Le Mercier I, Lines JL, Noelle RJ. Beyond CTLA-4 and PD-1, the generation Z of negative checkpoint regulators. *Front Immunol* 2015;6.
- [34] Sharpe AH, Wherry EJ, Ahmed R, Freeman GJ. The function of programmed cell death 1 and its ligands in regulating autoimmunity and infection. *Nat Immunol* 2007;8:239–45.
- [35] Prasad DVR, Nguyen T, Li Z, Yang Y, Duong J, Wang Y, et al. Murine B7–H3 Is a Negative Regulator of T Cells. *J Immunol* 2004;173:2500–6.
- [36] Podajil JR, Miller SD. Potential targeting of B7–H4 for the treatment of cancer. *Immunol Rev* 2017;276:40–51.
- [37] Chamian F, Lin S-L, Lee E, Kikuchi T, Gilleaudeau P, Sullivan-Whalen M, et al. Alefacept (anti-CD2) causes a selective reduction in circulating effector memory T cells (Tem) and relative preservation of central memory T cells (Tcm) in psoriasis. *J Transl Med* 2007;5:27.
- [38] Zhu Y, Paniccia A, Schulick AC, Chen W, Koenig MR, Byers JT, et al. Identification of CD112R as a novel checkpoint for human T cells. *J Exp Med* 2016;213:167–76.
- [39] Lu X, Liu J, Cui P, Liu T, Piao C, Xu X, et al. Co-inhibition of TIGIT, PD1, and Tim3 reverses dysfunction of Wilms tumor protein-1 (WT1)-specific CD8+ T lymphocytes after dendritic cell vaccination in gastric cancer. *Am J Cancer Res* 2018;8:1564–75.
- [40] Lupo KB, Matosevic S. CD155 immunoregulation as a target for natural killer cell immunotherapy in glioblastoma. *J Hematol Oncol* 2020;13.
- [41] Sakuishi K, Apetoh L, Sullivan JM, Blazar BR, Kuchroo VK, Anderson AC. Targeting Tim-3 and PD-1 pathways to reverse T cell exhaustion and restore anti-tumor immunity. *J Exp Med* 2010;207:2187–94.
- [42] Watanabe N, Gavrieli M, Sedy JR, Yang J, Fallarino F, Loftin SK, et al. BTLA is a lymphocyte inhibitory receptor with similarities to CTLA-4 and PD-1. *Nat Immunol* 2003;4:670–9.
- [43] Coles SJ, Wang ECY, Man S, Hills RK, Burnett AK, Tonks A, et al. CD200 expression suppresses natural killer cell function and directly inhibits patient anti-tumor response in acute myeloid leukemia. *Leukemia* 2011;25:792–9.
- [44] Coles SJ, Hills RK, Wang ECY, Burnett AK, Man S, Darley RL, et al. Expression of CD200 on AML blasts directly suppresses memory T-cell function. *Leukemia* 2012;26:2148–51.
- [45] Prendergast GC, Smith C, Thomas S, Mandik-Nayak L, Laury-Kleintop L, Metz R, et al. Indoleamine 2,3-dioxygenase pathways of pathogenic inflammation and immune escape in cancer. *Cancer Immunol Immunother* 2014;63:721–35.
- [46] Walunas TL, Lenschow DJ, Bakker CY, Linsley PS, Freeman GJ, Green JM, et al. CTLA-4 can function as a negative regulator of T cell activation. *Immunity* 1994;1:405–13.
- [47] Ehlerding EB, Lee HJ, Jiang D, Ferreira CA, Zahm CD, Huang P, et al. Antibody and fragment-based PET imaging of CTLA-4+ T-cells in humanized mouse models. *American journal of cancer research* 2019;9:53–63.
- [48] Huard B, Prigent P, Tournier M, Bruniquel D, Triebel F. CD4/major histocompatibility complex class II interaction analyzed with CD4- and lymphocyte activation gene-3 (LAG-3)-Ig fusion proteins. *Eur J Immunol* 1995;25:2718–21.
- [49] Fife BT, Pauken KE. The role of the PD-1 pathway in autoimmunity and peripheral tolerance. *Ann N Y Acad Sci* 2011;1217:45–59.
- [50] Agresta L, Hoebe KHN, Janssen EM. The emerging role of CD244 signaling in immune cells of the tumor microenvironment. *Front Immunol* 2018;9.
- [51] Kaye J. CD160 and BTLA: LIGHT's out for CD4+ T cells. *Nat Immunol* 2008;9:122–4.
- [52] Wolf Y, Anderson AC, Kuchroo VK. TIM3 comes of age as an inhibitory receptor. *Nat Rev Immunol* 2020;20:173–85.
- [53] Mittal D, Lepletier A, Madore J, Aguilera AR, Stannard K, Blake SJ, et al. CD96 is an immune checkpoint that regulates CD8+ T-cell antitumor function. *Cancer Immunol Res* 2019;7:559–71.
- [54] Manieri NA, Chiang EY, Grogan JL. TIGIT: A key inhibitor of the cancer immunity cycle. *Trends Immunol* 2017;38:20–8.
- [55] Cekic C, Linden J. Adenosine A2A Receptors Intrinsically Regulate CD8+ T Cells in the Tumor Microenvironment. *Cancer Res* 2014;74:7239–49.
- [56] Meissl K, Macho-Maschler S, Müller M, Strobl B. The good and the bad faces of STAT1 in solid tumours. *Cytokine* 2017;89:12–20.
- [57] Lee YS, Cho YB. CCL7 Signaling in the Tumor Microenvironment. *Adv Exp Med Biol* 2020;1231:33–43.
- [58] Li C, Jiang P, Wei S, Xu X, Wang J. Regulatory T cells in tumor microenvironment: new mechanisms, potential therapeutic strategies and future prospects. *Mol Cancer* 2020;19:116.
- [59] Mall C, Sckisel GD, Proia DA, Mirsoian A, Grossenbacher SK, Pai C-C-S, et al. Repeated PD-1/PD-L1 monoclonal antibody administration induces fatal xenogeneic hypersensitivity reactions in a murine model of breast cancer. *Onc Immunology* 2016;5:e1075114.
- [60] Smolle MA, Calin HN, Pichler M, Calin GA. Noncoding RNAs and immune checkpoints-clinical implications as cancer therapeutics. *FEBS J* 2017;284:1952–66.
- [61] Cortez MA, Ivan C, Valdecana D, Wang X, Peltier HJ, Ye Y, et al. PDL1 Regulation by p53 via miR-34. *J Natl Cancer Inst* 108 (2016) djv303-djv303.
- [62] Chen L, Gibbons DL, Goswami S, Cortez MA, Ahn Y-H, Byers LA, et al. Metastasis is regulated via microRNA-200/ZEB1 axis control of tumour cell PD-L1 expression and intratumoral immunosuppression. *Nat Commun* 2014;5:5241.
- [63] Schmid P, Adams S, Rugo HS, Schneeweiss A, Barrios CH, Iwata H, et al. *N Engl J Med* 2018;379:2108–21.
- [64] Chen L, Han X. Anti-PD-1/PD-L1 therapy of human cancer: past, present, and future. *J Clin Invest* 2015;125:3384–91.
- [65] Jazieh K, Bell R, Agarwal N, Abraham J. Novel targeted therapies for metastatic breast cancer. *Ann Transl Med* 2020;8.
- [66] Chan L-C, Li C-W, Xia W, Hsu J-M, Lee H-H, Cha J-H, et al. IL-6/JAK1 pathway drives PD-L1 Y112 phosphorylation to promote cancer immune evasion. *J Clin Invest* 2019;129:3324–38.
- [67] Hsu J-M, Li C-W, Lai Y-J, Hung M-C. Posttranslational modifications of PD-L1 and their applications in cancer therapy. *Cancer Res* 2018;78:6349–53.
- [68] Li C-W, Lim S-O, Xia W, Lee H-H, Chan L-C, Kuo C-W, et al. Glycosylation and stabilization of programmed death ligand-1 suppresses T-cell activity. *Nat Commun* 2016;7:12632.
- [69] Tu X, Qin B, Zhang Y, Zhang C, Kahila M, Newshean S, et al. PD-L1 (B7–H1) competes with the RNA exosome to regulate the DNA damage response and can be targeted to sensitize to radiation or chemotherapy. *Mol Cell* 2019;74:1215–1226.e1214.